Large Transient Shearing of Molten Polymers: Predictions of Rate-Dependent and Nonaffine Network Models

Y. Z. XU,* D. DE KEE,† and C. F. CHAN MAN FONG

Department of Chemical Engineering, University of Sherbrooke, Sherbrooke, Quebec, J1K 2R1, Canada

SYNOPSIS

Analytical expressions of shear stress evolution for arbitrary transient flows are obtained, based on a rate-dependent network (RDN) model as well as on a nonaffine network (NAN) model. Predictions of both models are evaluated for various step histories against experimental results on linear and branched polyethylene melts (LDPE and HDPE). Agreement with experiments justifies the usefulness of the computed stress functions regarding the predictions of shear responses in melt processing. A slow transient process is more adequately simulated by an NAN model than by an RDN model. The very slow reentanglement process following cessation of flow is poorly described by either model. This fact implies that additional relaxation mechanisms are involved. In the linear viscoelasticity of small deformation, elastic relaxation occurs. In processes involving large shear rates, additional parameters are needed to account for the structural changes accompanying the relaxation process. © 1995 John Wiley & Sons, Inc.

INTRODUCTION

Polymer melts are often assumed to have an entangled network structure. The modern concept of entanglement—topological constraints of chain contour tubes—leads to the reptation model of Doi and Edwards; the constitutive equation of this model takes the form of the K-BKZ equation.[1] In the K-BKZ equation, the stress is given in terms of the history of the strain only. It has been observed that in large and complex step flows the experimental results differ significantly from those predicted by the K-BKZ equation.[2-4] These large transient deformations are severe tests for constitutive equations.[5] In these flows, irreversible molecular processes are present and it might not be sufficient to consider the strain tensor only. The structural change of the network might depend on the shear as well as on the shear rate. Oldroyd pointed out that in flows that are subjected to a sudden change of stress or rate-of-strain the state of the stress does not depend on the strain tensor only.[6] It is desirable to include in the constitutive equation the history of the strain as well as that of the rate-of-strain.

We start with a constitutive equation for finite viscoelasticity, which may be written as

$$\boldsymbol{\tau} = -p\mathbf{I} + \int_{-\infty}^{t} m(t - t')\mathbf{G}(t, t')\, dt' \qquad (1)$$

where $\boldsymbol{\tau}$ is the stress tensor; p, the isotropic pressure; $\mathbf{I}$, the unit tensor; t, the present time; m, the memory function, and $\mathbf{G} = \mathbf{C}_t^{-1} - \mathbf{I}$, where $\mathbf{C}_t^{-1}$ is the relative Finger tensor.

The finite linear viscoelastic fluid predicts a constant shear viscosity and a zero secondary normal stress coefficient. To improve the model, we introduce a function of shear rate in eq. (1). By considering a network model in which the rate of change of network junctions depends on the shear rate, Carreau showed that the memory function in eq. (1) is a function of the invariants of the rate-of-strain.[7] This model, known as the rate-dependent network (RDN) model, can predict the viscosity function and the primary normal stress coefficient successfully.

* Permanent address: Institute of Chemistry, Academia Sinica, Beijing 100080, P.R. China.

† To whom correspondence should be addressed.

Journal of Applied Polymer Science, Vol. 55, 779–786 (1995)
 CCC 0021-8995/95/050779-08

An alternative approach is to allow slip to occur. Johnson and Segalman considered two corotational frames of reference.[8] One can be associated with the microstructure and the other with the macrostructure. By allowing nonaffine deformation between the two frames, they showed that the Finger tensor in eq. (1) has to be replaced by a generalized strain. A similar result is obtained by dropping the independent alignment in the Doi–Edwards model.[1,9] This model will be referred to as the nonaffine network (NAN) model.

These two approaches are not identical. We compared the shear stress responses of the two models for various forms of multi-rate-step flows. The prediction of shear stress in transient flows involving complex large strain and strain-rate histories is useful for many polymer processing operations, such as injection molding. Also, the comparison of model predictions with typical data for such complex deformation histories allows one to observe, e.g., that the shear history may drastically change the rheological properties. The preshearing effect reduces the melt elasticity as well as the viscosity in subsequent melt-forming operations. This "shear modification" can be used to improve melt processability. The mechanism associated with this effect can be attributed to a reentanglement time of the melt network. By using interrupted steps, it has been observed that the reentanglement time is much larger than is the characteristic time of the stress relaxation following steady flows. This may imply the existence of a kinetic mechanism related to entanglement evolution, in addition to the stress evolution due to linear viscoelasticity. In this article, we compare the experimental results on LDPE (E1) and HDPE (E2) with the theoretical predictions.

EQUATIONS OF SHEAR STRESS

We calculate the stress for a multi-rate-step history, as illustrated in Figure 1, for the two fluids mentioned earlier.

Rate-dependent Network (RDN) Model

The constitutive equation is given by

$$\tau = -p\mathbf{I} + \int_{-\infty}^{t} m[t - t', \Pi(t, t')]\mathbf{G}(t, t')\, dt' \quad (2)$$

We adopt the memory function proposed by De Kee and it can be written as[10]

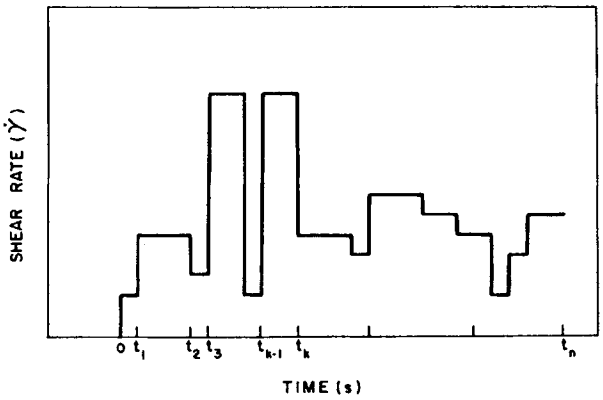

Figure 1 Multi-rate-step flow: $\dot{\gamma}$ vs. t.

$$m[t - t', \Pi(t, t')] = \sum_{p=1}^{n} \frac{\eta_p f_p[\Pi(t')]}{\lambda_p^2} \exp\left[-\int_{t'}^{t} \frac{dt''}{\lambda_p g_p[\Pi(t'')]}\right] \quad (3a)$$

$$f_p = f_0 \exp\{-(|\Pi|/2)^{1/2}(-2c + 3)t_p\} \quad (3b)$$

$$g_p = \exp\{-(|\Pi|/2)^{1/2}(c - 1)t_p\} \quad (3c)$$

In Eqs. (2) and (3a)–(3c), Π is the second invariant of the rate-of-deformation tensor, and η_p and λ_p are constants that have dimensions of viscosity and time, respectively. c is a dimensionless constant and we assume t_p to be equal to λ_p. The dimensionless parameter f_0 can be assumed to be equal to 1 in flows where the deformation is small. For large deformations, it can differ from 1.

For the arbitrary multi-rate-step history shown in Figure 1, the shear stress $\tau(t)$ at the present time is the sum of the stress contributions due to the deformations in past times. We divide the past times into intervals (t_{k-1}, t_k), $k = 0, 1, \ldots, n$. A constant shear rate $\dot{\gamma}_k$ is applied in the interval (t_{k-1}, t_k). We let t_{-1} be $-\infty$, t_0 be zero, and t_n be the present time t. $\tau(t)$ can then be written as

$$\tau(t) = \sum_{k=0}^{n} I_k \quad (4)$$

where I_k is the contribution to $\tau(t)$ due to the deformation in the interval (t_{k-1}, t_k) and is given by

$$I_k = \sum_{p=1}^{m} \frac{\eta_p f_{p,k}}{\lambda_p} \exp\left[\sum_{i=k}^{n-1} \frac{t_i}{\lambda_p}\left(\frac{1}{g_{p,i+1}} - \frac{1}{g_{p,i}}\right)\right] \times \left\{g_{p,k}\left[\sum_{i=k}^{n-1} t_i(\dot{\gamma}_i - \dot{\gamma}_{i+1}) + \dot{\gamma}_n t_n\right]\right.$$

$$\times \left(\frac{t_k}{e^{\lambda_p g_{p,k}}} - \frac{t_{k-1}}{e^{\lambda_p g_{p,k}}} \right) - \frac{\dot{\gamma}_k g_{p,k}}{e^{\lambda_p g_{p,k}}}$$

$$\times [(t_k - t_{k-1})(t_k + t_{k-1} - \lambda_p g_{p,k})] \Bigg\} - \frac{t}{e^{\lambda_p g_{p,n}}} \quad (5)$$

Nonaffine Network (NAN)

The constitutive equation can be written as

$$\tau = -p\mathbf{I} + \int_{-\infty}^{t} G(t - t')\mathbf{E}(t, t') \times \mathbf{D}^*(t')\mathbf{E}^{\dagger}(t, t')\, dt' \quad (6a)$$

where † refers to the transpose

$$G(t - t') = \sum_{p=1}^{m} G_p e^{-(t-t')/\lambda_p} \quad (6c)$$

$$\mathbf{D}^* = a(\Pi)\mathbf{D} \quad (6b)$$

$$\frac{\partial \mathbf{E}}{\partial t} = \mathbf{A}(t) \cdot \mathbf{E}(t, t'), \mathbf{E}(t', t') = \mathbf{I} \quad (6d,e)$$

$$\mathbf{A} = \mathbf{L} - (1 - a)\mathbf{D} \quad (6f)$$

L and **D** are the velocity gradient and the rate-of-deformation tensor, respectively, in the nonslipping frame. a is the slip parameter and is equal to 1 when there is no slip.

The shear stress $\tau(t)$ is given by

$$\tau(t) = \sum_{k=1}^{\infty} S_k \quad (7)$$

where S_k is the contribution to $\tau(t)$ due to the deformation imposed during the interval (t_{k-1}, t_k).

It is shown in the Appendix that S_k is given by

$$S_k = \frac{a_k \dot{\gamma}_k}{2} \sum_{p=1}^{m} \frac{G_p e^{-t/\lambda_p}}{\lambda_p^{-2} + \beta_k^2} [e^{t_k/\lambda_p} \{ \lambda_p^{-1} \cos(\alpha_k - \beta_k t_k) - \beta_k \sin(\alpha_k - \beta_k t_k) \} - e^{(t_{k-1})/\lambda_p} \{ \lambda_p^{-1} \cos(\alpha_k - \beta_k t_{k-1}) - \beta_k \sin(\alpha_k - \beta_k t_{k-1}) \}] \quad (8a)$$

where

$$\alpha_k = 2\xi_k \left\{ \sum_{i=k+1}^{n} \dot{\gamma}_i (t_i - t_{i-1}) + \dot{\gamma}_k t_k \right\} \quad (8b)$$

$$\beta_k = 2\xi_k \dot{\gamma}_k \quad (8c)$$

$$\xi_k = \sqrt{1 - a_k^2} \quad (8d)$$

MATERIALS AND CHARACTERIZATION

The data on polyethylene (PE) (E1)-resin 10 (low-density polyethylene [LPPE]) and (E2)-resin 22 (high-density polyethylene [HDPE]) are available.[11] All rheological measurements for PE were performed at 443 K.

The linear relaxation time spectra are obtained from the dynamic moduli G' and G'' by using Tschoegl's second approximation. A set of discrete values of relaxation times λ_p and moduli G_p are selected from the continuous spectrum as listed in Table I. λ_p and G_p were used to calculate G' and G'' from the equations of a generalized Maxwell model.

Some rheological data of the samples were presented.[11] The η_p values of the RDN model can be obtained as follows:

$$\eta_p = G_p \lambda_p \quad (9)$$

EVALUATION OF MODELS USING COMPLEX TRANSIENT SHEARING

Reduction in Shear Rate

In this experiment, the fluid is subjected to a shear rate $\dot{\gamma}_1$ for a sufficiently long time such that the steady state is reached. The shear rate is then suddenly reduced to $\dot{\gamma}_2$ and is kept at this value for a long time. Finally, the sample is no longer sheared. The shear stress is measured all along.

Dealy and Tsang reported data on this type of experiment on the E1 and E2 melts mentioned earlier.[12] They related their observations to the struc-

Table I Discrete Spectra for PE Samples at 443 K

	Sample	
Relaxation Time λ_p (s)	E1 G_p (Pa)	E2 G_p (Pa)
0.00316	20954	
0.01	15895	31715
0.0316	11783	26379
0.1	8342	19782
0.316	5386	13221
1.0	3245	7966
3.16	1703	4086
10.0	797.6	1703
31.6	317.2	590.6
100.0	8.54	166.5

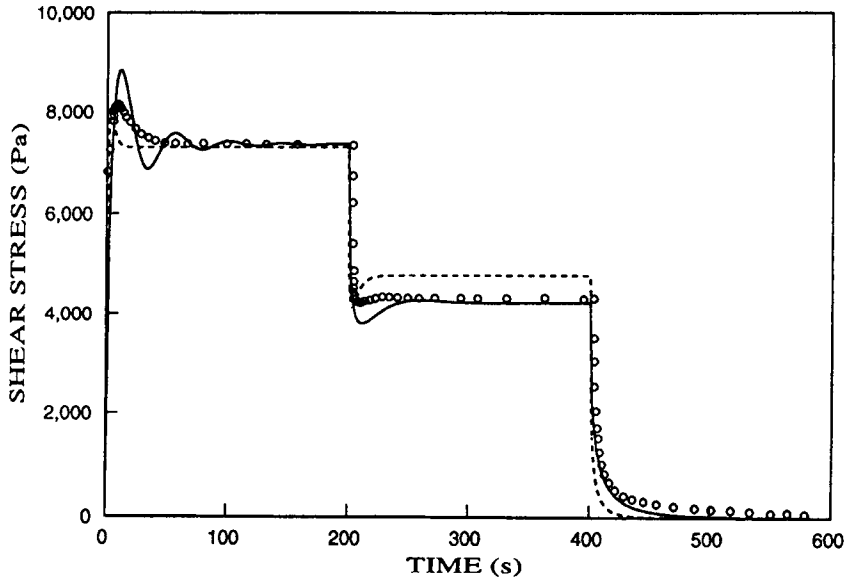

Figure 2 Stress growth, reduction in shear rate, ($\dot{\gamma}_1 = 0.64\ s^{-1}$, $\dot{\gamma}_2 = 0.258\ s^{-1}$), and stress relaxation curves for the E1 melt. The experimental data are from Tsang.[15] The broken line represents the prediction of the RDN model ($c = 1.5$ and $f_0 = 1.48$). The solid line is that of the NAN model ($a = 0.994$). The material parameters are given in Table I.

ture rebuilding following the reduction in shear rate. They compared their data with the predictions of the Acierno et al. and Phan-Thien and Tanner models.[13,14]

Figure 2 shows qualitative between data and model predictions for the RDN and the NAN models. To allow the NAN model to predict the data, it was necessary to multiply the G_p values by a constant factor of 1.65. Both models predict stress overshoot and undershoot in qualitative agreement with the experimental data. The magnitude of the stress overshoot and undershoot predicted by the NAN model is greater than the experimentally observed one. For the RDN model, once the material parameters have been chosen to fit the stress at $\dot{\gamma}_1$, the predicted stress for $\dot{\gamma}_2$is higher than the measured one.

Figure 3 shows the results for the HDPE (E2) sample. Qualitatively, they are similar to those shown in Figure 2. However, quantitatively, they are better. In Figure 2, the NAN model predicts stress oscillation that is not observed experimentally. This stress oscillation is due to the sin and cos terms in eq. (8a), which is also associated with nonaffine deformation. By considering only one mode and by a suitable choice of material parameters, it is possible to reduce the amplitude of the oscillation to such an extent that it becomes negligible. Thus, in Figure 3, we do not observe stress oscillation for the NAN model. We used two modes to calculate the stress for the RDN model and it can be seen that overall the predictions are in good agreement with the experimental data.

In Figure 4, we replotted the experimental data given in Figure 2 with the predictions of the NAN model using only one mode. In this case, the calculated stress shows no oscillation and the agreement between the theoretical and experimental values is better than that shown in Figure 2.

We explored the effect of changing the values of a in the NAN model and the form of the spectrum in the RDN model. No significant change was observed. In all cases (Figs. 2–4), it is predicted that the stress attains its steady value from its maximum value in a time shorter than the one observed experimentally.

Interrupted Shear Flow

In this experiment, a constant shear rate $\dot{\gamma}$ is applied and maintained until the steady state is reached. The shearing is then stopped and the fluid is allowed to rest for a period t_r. It is then sheared again at the same shear rate $\dot{\gamma}$. This process of shearing and resting for various values of t_r is repeated. The maximum value of the shear stress τ_m, which is a function of t_r is recorded. This is schematically shown in Figure 5.

Stratton and Butcher suggested that such an experiment can be used to provide an estimate of the

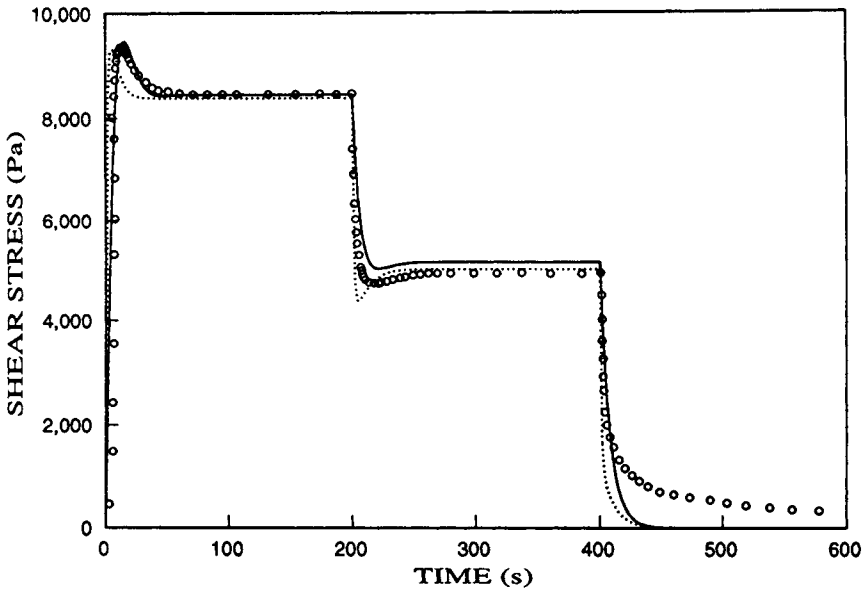

Figure 3 Stress evolution in a reduced step flow ($\dot{\gamma}_1 = 0.258\ s^{-1}$, $\dot{\gamma}_2 = 0.104\ s^{-1}$) for the E2 melt. Comparison of measured data with predictions of the one-mode NAN model ($G_1 = 14000$ Pa, $\lambda_1 = 8$ s, $a = 0.98$) and the two-mode RDN model ($\eta_1 = \eta_2 = 38000$ Pa-s, $\lambda_1 = 1$ s, $\lambda_2 = 10$ s, $c = 1.35$). Solid line: NAN model; dotted line: RDN model.

reentanglement time.[16] We define the reduced stress recovery S_r by

$$S_r = \frac{\tau_m(\infty, \dot{\gamma}) - \tau_m(t_r, \dot{\gamma})}{\tau_m(\infty, \dot{\gamma}) - \tau_s(\dot{\gamma})} \qquad (10)$$

where $\tau_m(\infty, \dot{\gamma})$ is the maximum shear stress initially (assuming that initially the fluid has been in a state of rest for an infinite period) and τ_s is the steady value of the shear stress.

In Figure 6, we plotted the predicted and experimental values of S_r as a function of t_r. The experimental values are for the E2 sample.[12] It can be seen that the agreement between the theoretical and experimental values is poor. A similar deviation was obtained by Dealy and Tsang.[12] The present test

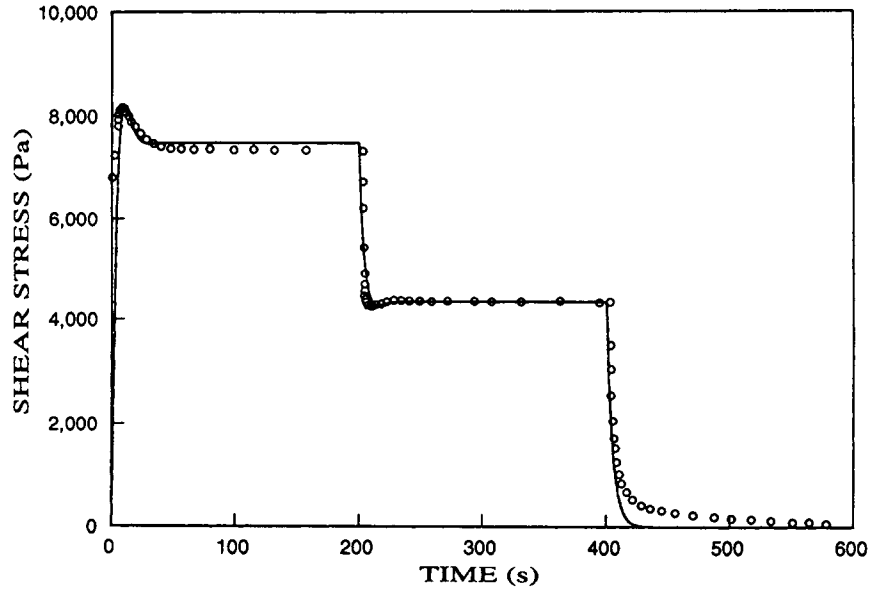

Figure 4 Stress evolution in reduced shear step for the E1 melt. Comparison with the one-mode NAN model ($G_1 = 7400$ Pa, $\lambda_1 = 5$ s, $a = 0.993$). Experimental data as in Figure 2.

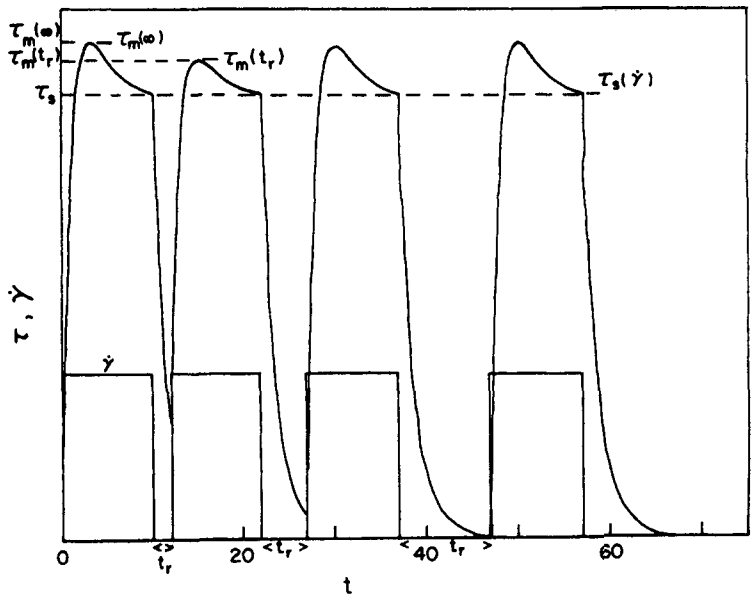

Figure 5 Interrupted flow. τ and $\dot\gamma$ vs. t.

highlights the discrepancy observed earlier, which is that the time taken for the stress to reach its steady value is predicted to be shorter than the observed one.

CONCLUSIONS

The RDN model predicts the transient properties qualitatively. The relaxation is too fast and the peaks are too narrow. This may be attributed to the relatively sharp exponential rate dependence. The NAN model yields a better quantitative response but predicts oscillatory behavior. This problem can be eliminated by a suitable choice of one relaxation mode. The stress relaxation following cessation of flow becomes realistic when the slip factor a is unity. The transient response at given shear rate is not sensitive to the whole spectrum. The prediction of

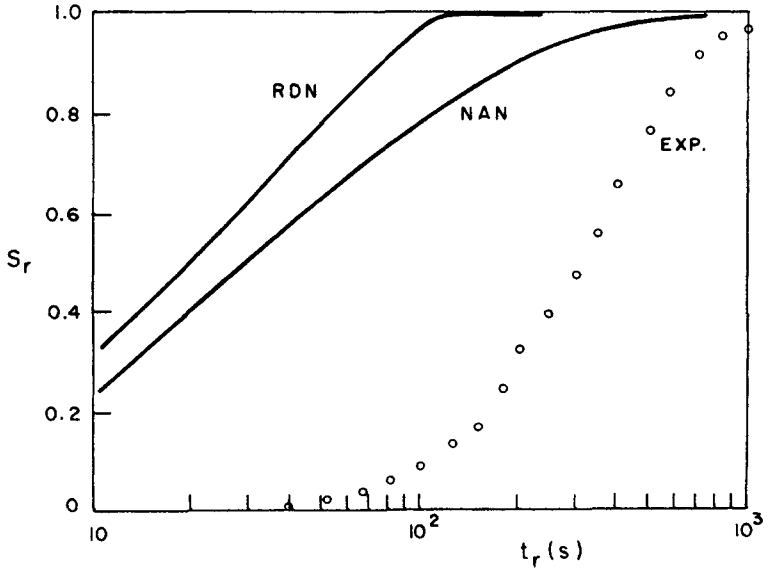

Figure 6 S_r vs. t_r for E2 melt at 443 K. Theoretical predictions based on complete spectrum (Table I). c = 1.35 (RDN model). a = 0.99 (NAN model).

both models cannot substantially be improved by broadening the spectrum. Also, the change of spectrum is limited by the predictions of the steady flow curves.

The slip factor seems to play an important role in the nonlinear response. The predicted oscillations are most likely due to the tumbling of the flow units in the shear field.[9] But the fact that a single mode rather than a broad spectrum can dampen the oscillations implies that the reasons for the oscillations might not be fully understood.

The interrupted flow experiment represents a critical test for the entanglement dynamics. The predicted value of the reentanglement time is about one decade lower than the measured one. The discrepancy is not so severe in the case of noninterrupted shear steps. This implies that there exists some mechanism of reentanglement that has not been considered in the current models.

D. De Kee wishes to acknowledge financial support from the Natural Sciences and Engineering Research Council of Canada. Also, the award of an NSERC International Scientific Exchange Award made Y.Z.X.'s participation possible.

APPENDIX

The velocity distribution for a simple shear flow is given by

$$V_1 = \dot{\gamma} x_2, \quad V_2 = V_3 = 0 \tag{A.1}$$

The tensors **A** and **D*** are given by [eqs. (6c) and (6f)]

$$\mathbf{D}^* = \frac{a}{2}\begin{bmatrix} 0 & \dot{\gamma} & 0 \\ \dot{\gamma} & 0 & 0 \\ 0 & 0 & 0 \end{bmatrix} \tag{A.2}$$

$$\mathbf{A} = \dot{\gamma}\begin{bmatrix} 0 & 1 & 0 \\ 0 & 0 & 0 \\ 0 & 0 & 0 \end{bmatrix} - \frac{(1-a)}{2}\begin{bmatrix} 0 & \dot{\gamma} & 0 \\ \dot{\gamma} & 0 & 0 \\ 0 & 0 & 0 \end{bmatrix} \tag{A.3}$$

From eqs. (6d) and (6e), we can obtain **E**, which is substituted in eq. (6a) to obtain an expression for the stress τ. It is found that the shear stress $\tau(t)$ is given by

$$\tau = \frac{a}{2}\int_{-\infty}^{t} G(t-t')\dot{\gamma}(t')\cos(2\xi\sigma)\,dt' \tag{A.4a}$$

where

$$\xi = \sqrt{1-a^2} \tag{A.4b}$$

$$\sigma = \int_{t'}^{t} \dot{\gamma}\,dt'' \tag{A.4c}$$

S_k is the contribution to $\tau(t)$ due to the imposed shear rate $\dot{\gamma}_k$ in the interval $t_{k-1} < t < t_k$ and can be written as

$$S_k = \frac{a_k}{2}\int_{t_{k-1}}^{t_k} G(t-t')\dot{\gamma}_k\cos(2\xi_k\sigma_k)\,dt' \tag{A.5a}$$

where

$$\xi_k = \sqrt{1-a_k^2} \tag{A.5b}$$

$$\sigma_k = \sum_{i=k+1}^{n} \dot{\gamma}_i(t_i - t_{i-1}) + \dot{\gamma}_k(t_k - t') \tag{A.5c}$$

and a_k is the value of a in the interval $t_{k-1} < t < t_{k+1}$. Substituting eq. (6b) into eq. (A4a) and making use of the formula

$$\int e^{ax}\cos bx\,dx = \frac{e^{ax}}{a^2+b^2}(a\cos bx + b\sin x) \tag{A.6}$$

we obtain eq. (8a).

REFERENCES

1. M. Doi and S. F. Edwards, *The Theory of Polymer Dynamics*, Oxford University Press, New York, 1986.
2. K. Osaki and M. Kurata, *Macromolecules*, **13**, 671 (1980).
3. K. Osaki, S. Kimura, and M. Kurata, *J. Rheol.*, **25**, 549 (1981).
4. C. M. Vrentas and W. W. Graessley, *J. Rheol.*, **26**, 359 (1982).
5. J. M. Dealy and K. F. Wissbrun, *Melt Rheology and Its Role in Plastic Processing. Theory and Applications*, Van Nostrand Reinhold, New York, 1990.
6. J. G. Oldroyd, *Proc. R. Soc. A*, **283**, 115 (1965).
7. P. J. Carreau, *Trans. Soc. Rheol.*, **16**, 99 (1972).

8. M. W. Johnson and D. Segalman, *J. Non-Newtonian Fluid Mech.*, **2,** 255 (1977).
9. R. G. Larson, *Constitutive Equations for Polymer Melts and Solutions,* Butterworths, New York, 1988.
10. D. De Kee, PhD Thesis, University of Montreal, Montreal, Quebec, 1977.
11. W. K. W. Tsang and J. M. Dealy, *J. Non-Newtonian Fluid Mech.*, **9,** 203 (1981).
12. J. M. Dealy and W. K. W. Tsang, *J. Appl. Polym. Sci.*, **26,** 1149 (1981).
13. D. Acierno, F. P. La Mantia, G. Marrucci, and G. Titomanlio, *J. Non-Newtonian Fluid Mech.*, **1,** 125 (1976).
14. N. Phan-Thien and R. I. Tanner, *J. Non-Newtonian Fluid Mech.*, **2,** 353 (1977).
15. W. K. W. Tsang, PhD Thesis, McGill University, Montreal, Quebec, 1980.
16. R. A. Stratton and A. F. Butcher, *J. Appl. Polym. Sci.*, **11,** 1747 (1973).

Received May 11, 1994
Accepted August 23, 1994